Electronic Supplementary Material (ESI) for Chemical Communications.

High-resolution sub-cellular imaging by correlative nanoSIMS and EM of amiodarone internalisation by lung macrophages as the evidence for drug-induced phospholipidosis.

Haibo Jiang [a]*, Melissa K. Passarelli[b], Peter M. G. Munro[c], Matt R. Kilburn [a], Andrew West[d], Colin T. Dollery[d], Ian S. Gilmore[b], Paulina D. Rakowska[b]*

[a]Centre for Microscopy, Characterisation and Analysis, University of Western Australia, 35 Stirling Highway, Crawley WA 6009, Australia. *E-mail: Haibo.Jiang@uwa.edu.au
[b]National Centre of Excellence in Mass Spectrometry Imaging (NiCE-MSI), National Physical Laboratory, Hampton Road, Teddington, Middlesex, TW11 0LW, UK. *E-mail: Paulina.Rakowska@npl.co.uk
[c]Institute of Ophthalmology, University College London, Bath Street, London, EC1V 9EL, UK.
[d]GlaxoSmithKline, Gunnels Wood Road, Stevenage, Hertfordshire, SG1 2NY, UK.

Experimental Protocols:

Cell Culture: NR8383 cells, an immortalized cell line derived from a lung macrophage (Sprague−Dawley rat), were grown in 25 cm^3 Nunc EasYFlask (Thermo Scientific, U.S.A.) with Ham's F-12 Nutrient Mixture medium containing GlutaMax and Phenol Red (Gibco, U.S.A.) and 15% dialyzed, heat-inactivated fetal bovine serum (Gibco, U.S.A.). The 5 mg/ mL stock solutions of amiodarone hydrocholoride (Sigma-Aldrich, CAS 19774−82−4, purity ≥98%) was prepared in 50:50 water/MeOH. The stock solution was added to the growth medium for a final medium concentration of 1.56 µg/mL. The cells were incubated (5% CO_2 and 37 °C) in the drug doped medium solution for 72 h.

TAG fixation and embedding: Cells were flat-embedded by fixing, in situ, in the 25 cm^3 flasks (Nunc EasYFlask (Thermo Scientific, U.S.A.)) with a mixture of 2.5% glutaraldehyde and 0.5 % tannic acid buffered to pH 7 with 0.8M sodium cacodylate (overnight at room temperature). After two rinses in cacodylate buffer (pH 7.4) cells were treated for 2 hours in aqueous 1% osmium tetroxide, rinsed twice in deionised water, dehydrated by passage through ascending alcohols (50, 70, 90 and 4 x 100%, 10 mins each step) and the flask filled with araldite CY212 resin which was cured overnight at 60˚C.

Analytical sample preparation: 500 nm thick sections were cut with a (Diatome) diamond knife on an Ultramicrotome. The sections were placed on a 15 nm platinum coated coverslip and air dry at 60 degrees.

Electron microscopy:
500 nm sections were then transferred to a FEI Verios Scanning Electron Microscopy for imaging using the through-the-lens (TLD) detector for backscattered electrons (BSE). BSE images were taken with a 1 kV incident beam with 0.1 nA current and ~ 2 mm working distance. Sections were then coated with 5 nm of platinum in a SC 7640 Polaron sputter coater to render the surface conductive for NanoSIMS imaging.

NanoSIMS imaging and data processing:
The 16keV Cs^+ primary beam in the NanoSIMS was first used to remove the platinum on the surface at selected locations, and at the same time implanted a Cs^+ dose of ~1.0×10^{17} atoms/cm^2 to reach the steady state of secondary ion signals for NanoSIMS imaging. A small aperture (D1 = 3) is used for

imaging single cells to match the primary beam size and the pixel size. The instrument was tuned for $^{12}C^{14}N^-$, $^{31}P^-$ and $^{127}I^-$ ions to give morphological information and distribution of amiodarone. NanoSIMS images were collected with a dwell time of 30,000 µs/pixel each frame for 256 × 256 pixels or 512 × 512 pixels images and processed with OpenMIMS plugin (MIMS, Harvard University; www.nrims.harvard.edu) in ImageJ. Areas of interest were drawn pixel by pixel in the $^{127}I^-$ enriched areas, and total counts of $^{127}I^-$ and $^{31}P^-$ in these areas were extracted. 3D $^{31}P^-$ and $^{127}I^-$ NanoSIMS images were drift corrected by OpenMIMS and reconstructed from 22 frames of NanoSIMS imaging on the same area.

Additional data:

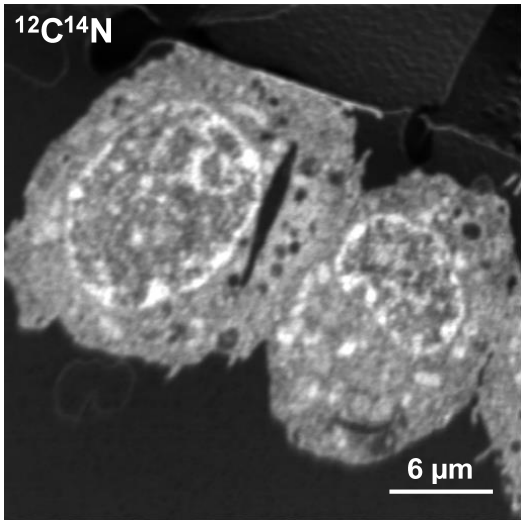

Figure S-1. $^{12}C^{14}N^-$ NanoSIMS images of the same area shown in Figure 1 of the main manuscript. Relatively lower $^{12}C^{14}N^-$ secondary ion intensities are observed in the $^{127}I^-$ enriched areas.

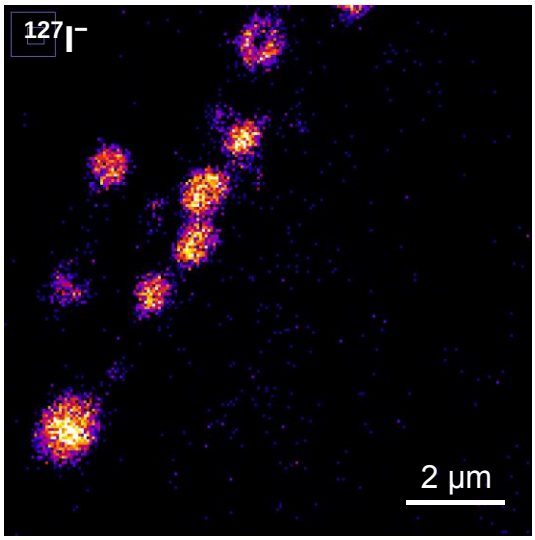

Figure S-2. Only low signal of iodine $^{127}I^-$ dispersed the cytosol is detected outside of the lysosomes. The intensity of the $^{127}I^-$ signal inside the lysosomes is around 10-14 counts whilst outside it is around 1-3.

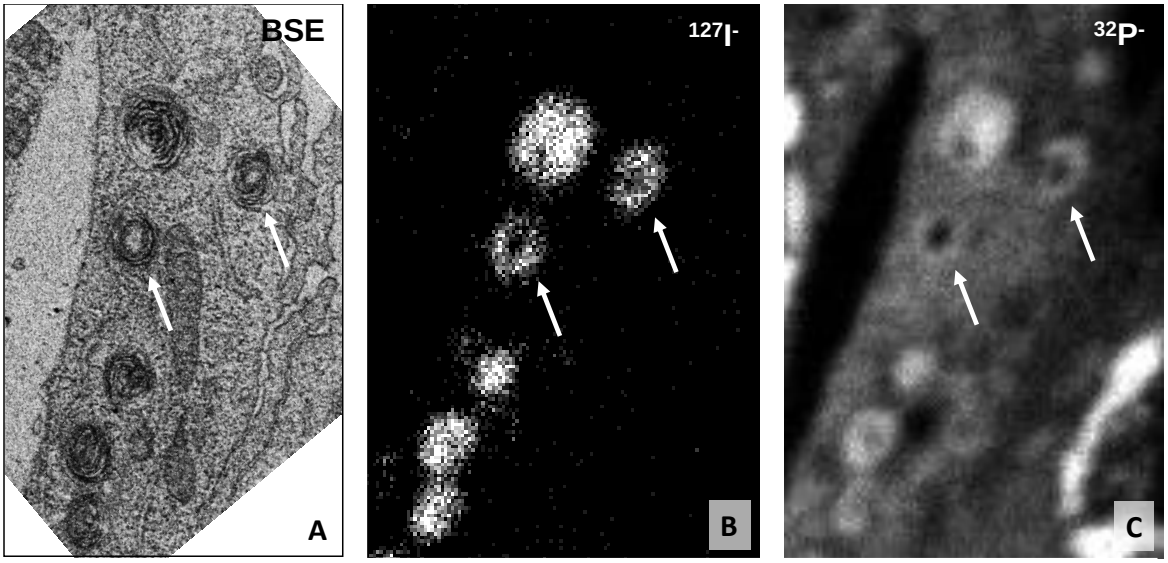

Figure S-3. Imaging at sub-organelle level showing the iodine ($^{127}I^-$) associated at a high relative concentration with phospholipids ($^{32}P^-$) in the MLLs. Iodine is clearly absent from the internal regions of the MLLs that do not contain the phospholipids (examples indicated by arrows). The images are zoomed fragments of the ones in Figure 1 of the main manuscript.

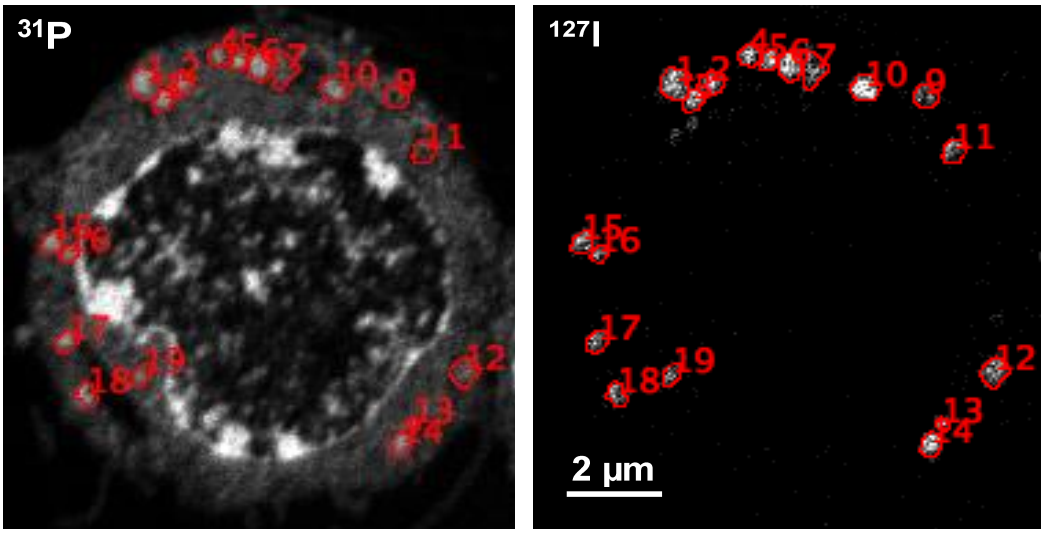

Figure S-4. Example of quantitative assessment of $^{127}I^-$ and $^{31}P^-$ ion signals. Areas of interest were drawn pixel by pixel and $^{127}I^-$ and $^{31}P^-$ secondary ion counts were extracted from each area.

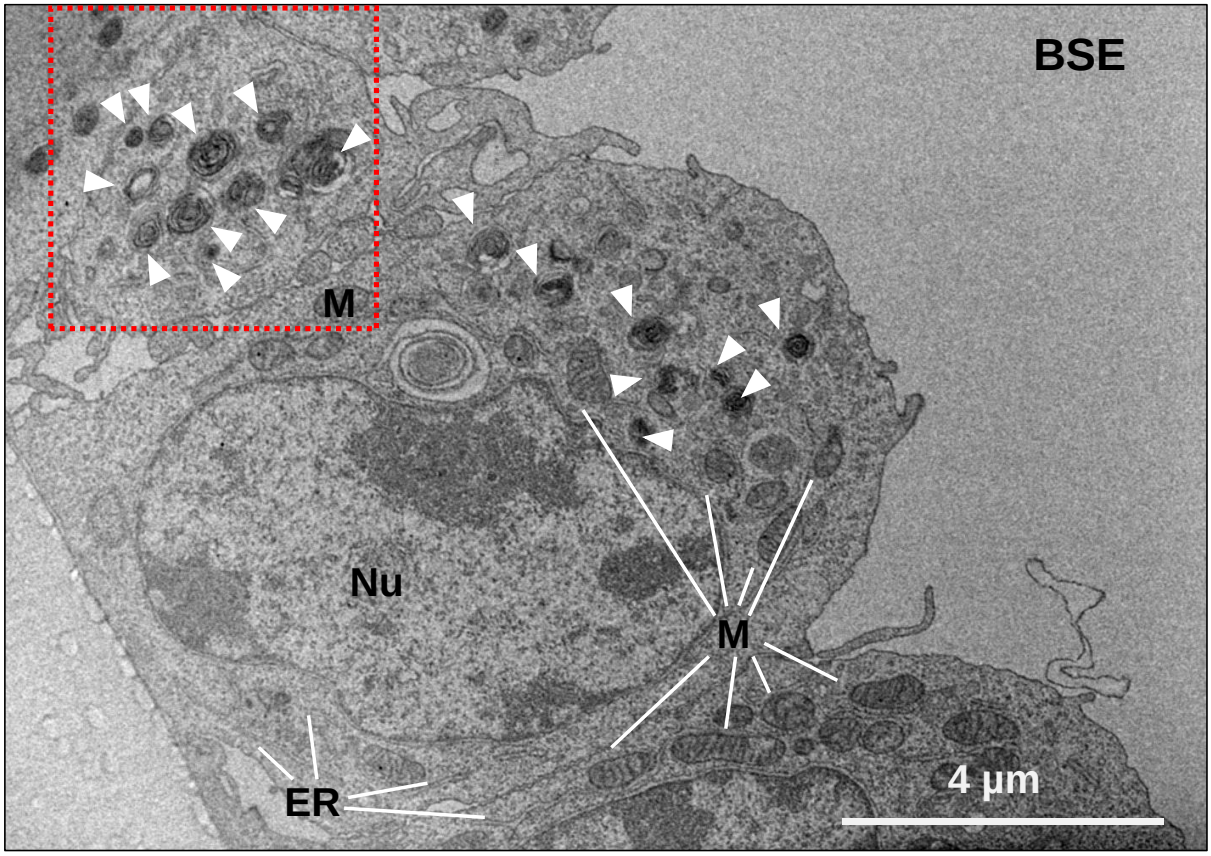

Figure S-5. BSE micrograph revealing the presence of the multilammelar lysosomes (arrows) among other cellular compartments (Nu = nucleus, M = mitochondria, ER = endoplasmic reticulum). Red marking indicates the area examined in Figure 2 of the main manuscript.